

## Synthesis of Silver Nanoparticles of Corn Silk Agrowaste and Their Bioactivities

S. FULORIA<sup>1</sup>, O.J. HONG<sup>1</sup>, C.B. KIM<sup>1</sup>, B.Y.S. TING<sup>1</sup>, S. KARUPIAH<sup>1</sup>, N. PALIWAL<sup>1</sup>,  
U. KUMAR<sup>2</sup>, K. SATHASIVAM<sup>3</sup>, S. VETRISELVAN<sup>4</sup> and N.K. FULORIA<sup>1,\*</sup>

<sup>1</sup>Pharmaceutical Chemistry Unit, Faculty of Pharmacy, AIMST University, Kedah 08100, Malaysia

<sup>2</sup>Department of Physiology, Faculty of Medicine, AIMST University, Kedah 08100, Malaysia

<sup>3</sup>Department of Biotechnology, Faculty of Applied Sciences, AIMST University, Kedah 08100, Malaysia

<sup>4</sup>Faculty of Medicine, MAHSA University, Bandar Saujana Putra, 42610, Selangor, Malaysia

\*Corresponding author: Fax: +60 44 298007; Tel: +60 16 4037685; E-mail: [nfuloria@gmail.com](mailto:nfuloria@gmail.com)

Received: 6 January 2020;

Accepted: 18 March 2020;

Published online: 30 May 2020;

AJC-19903

Present study was intended to synthesize silver nanoparticles (AgNPs) using corn silk aqueous extract (CSAE) and evaluate for antimicrobial and antiurolithiatic potential. The aqueous decoction of corn silk offered light yellow CSAE. Treatment of AgNO<sub>3</sub> with CSAE offered AgNPs with absorbance 430 nm. Optimization study established 5 mM silver nitrate, 2.5:7.5 extract to AgNO<sub>3</sub> ratio, pH 8, and 24 h time as parametric requirement for synthesis of AgNPs using CSAE. Stability study supported the AgNPs stability based on retention of SPR signal between 428 to 450 nm. The synthesis of AgNPs was confirmed on broad and shifted FTIR bands; XRD signals at 2θ values of 32.27°, 40.72°, 46.20°, 65.69°, 69.31° and 76.49° indexed to 111, 200, 220 and 311 planes, respectively; particle size range from 22.05-36.69 nm in FESEM; and elemental silver content of 62.17% as per EDX spectrum. The synthesized AgNPs exhibited high antibacterial and antiurolithiatic potential. Present study recommends that synthesis of AgNPs using CSAE is a facile and eco-friendly method.

**Keywords:** Silver nanoparticles, Corn silk, Urolithiasis, Antibacterial activity.

### INTRODUCTION

The painful urolithiasis disorder involves formation of stones *via* polycrystalline concretions in the kidney, urinary bladder, or urethra. Renal calculi (kidney stones) mainly consist of calcium are formed when the urine is supersaturated with salt and minerals such as calcium oxalate, uric acid, ammonium magnesium phosphate (struvite) and cysteine [1]. Unavailability of proper conventional therapeutic treatments for kidney stone and side effects associated with surgery motivates the investigators to search natural remedies that can remove larger stones [2]. The urinary tract infections caused by gram positive and negative bacteria are known to enhance the chances of stones formation [3]. Research suggests extensive administration of conventional antibiotics offer several shortcomings, such as: prolonged treatment, multiple drug resistance (MDR), and high mortality risk [4]. Current decade witnesses enormous research over metallic nanoparticles, especially over silver nanoparticles (AgNPs).

The AgNPs suppress the drug resistance and augment the antimicrobial potential of chemical moieties against various pathogens like *E. coli*, *S. aureus*, *K. pneumoniae* and *B. cereus* [4-9]. There are several ways to synthesize metallic nanoparticles, such as heat evaporation, chemical reduction, electrochemical reduction and microwave irradiation. But synthesis of AgNPs by these methods needs surface passivators (like thiophenol, mercapto acetate and thiourea) that may pollute the environment [4,10]. The chemical synthesis of AgNPs may cause adsorption of toxic entities on the particles surface, which manifest in adverse effects on administration. Hence, search for a method that presents higher environmental safety, economy, non-toxicity, and yield is a serious concern for the researchers.

The synthesis of nanoparticles using plant materials is considered as green. The nanoparticles green synthesis offers several benefits, such as environmental friendliness, simplicity, cost-effectiveness, stability and reproducibility [11-13]. Studies report corn silk (an agrowaste of *Zea mays*) to possess anti-oxidant [14], antimicrobial [15], diuretic [16] and nephropro-

fective [17] activities. Evidences suggest that the potency of corn silk to inhibit bacteria and calcium oxalate crystals growth could be augmented by blending into AgNPs. Hence, present study was intended to perform synthesis of AgNPs using corn silk and evaluate their antibacterial and antiurolithiatic potential. Present study involved corn silk aqueous extract (CSAE) preparation using decoction; and AgNPs synthesis (using CSAE), optimization (by UV-visible spectrometry), stability study (using UV-visible spectrometry), characterization (FTIR, XRD, FESEM and EDX analysis), antimicrobial evaluation against pathogenic bacteria (well-diffusion method) and *in vitro* antiurolithiatic evaluation against crystal growth inhibition (nucleation assay).

## EXPERIMENTAL

**Preparation of corn silk aqueous extract:** Whole corn (*Zea mays*) was procured from the province of Sungai Petani, Malaysia. Silky hairs (*Stigma maydis*) were collected from each fruit, washed (to remove impurities/dirt), dried for 24 h at 40 °C and finally powdered. Accurately weighed 25 g of corn silk powder was added to 400 mL of deionized water and boiled for 15 min with continuous stirring. Mixture was cooled to room temperature, filtered and filtrate was centrifuged at 5000 rpm for 15 min. Supernatant liquid of corn silk aqueous extract (CSAE) was collected and stored in refrigerator at 4 °C for further use.

**Synthesis of AgNPs:** The synthesis of AgNPs was performed by following protocol with slight modification [18]. Briefly, in a 100 mL volumetric flask 25 mL of CSAE and 75 mL of 5 mM AgNO<sub>3</sub> solution were added and mixed well. The flask was wrapped with aluminium foil (to prevent photolysis). The pH of the mixture was adjusted to pH 8 by adding 0.1 N NaOH solution. The mixture was kept in dark at room temperature for 24 h. The change in colour of solution from golden yellow to dark brown indicated the reduction of silver nitrate to silver nanoparticles. The mixture was centrifuged at 5000 rpm for 90 min. The supernatant layer was discarded to offer crude AgNPs pellet. The crude AgNPs pellet was rewashed (repeatedly 2 to 3 times) with deionized water, re-centrifuged and finally air dried to yield pure AgNPs.

**UV-visible analysis:** The successful synthesis of AgNPs was confirmed by UV-visible spectrometry. The UV visible analysis was conducted according to reported protocol with minor modifications [19]. Briefly, in a 10 mL volumetric flask, 1 mg of dried AgNPs was dissolved in 9 mL of deionized water. Finally, the volume was made up to 10 mL and test mixture was subjected to UV-visible analysis at room temperature to detect the surface plasmon resonance (SPR) signal. The measurement was made at 200 to 800 nm using Shimadzu U-2800 spectrophotometer running at a scanning speed of 300 nm/min. The UV-visible absorption spectrum of AgNPs determined the reduction of Ag<sup>+</sup> ions.

**Optimization of AgNPs synthesis:** The synthesis of AgNPs was optimized using UV-visible studies over CSAE and silver nitrate reaction mixture maintained under different parametric conditions, such as volumetric ratio of CSAE to AgNO<sub>3</sub>, concentration of AgNO<sub>3</sub>, pH, temperature and stability studies with time required for synthesis of AgNPs. Optimization

was performed as per reported protocols with minor modifications [4,18].

**Optimization based on concentration of AgNO<sub>3</sub>:** The four different concentrations of AgNO<sub>3</sub> (1, 2, 3 and 5 mM) were used for AgNPs synthesis. The four reaction mixtures were subjected to visual examination (for monitoring of colour change from yellow to brown) and UV-visible spectrometry (for observation of SPR signal in UV-visible spectrum) to determine the ideal concentration of AgNO<sub>3</sub> required for synthesis of pure AgNPs.

**Optimization based on volumetric ratio of CSAE to AgNO<sub>3</sub>:** The five different volumetric ratios of CSAE to AgNO<sub>3</sub> (1:9, 1.5:8.5, 2:8, 2.5:7.5 and 5:5) were used for AgNPs synthesis. All five reaction mixtures were subjected to visual examination (to observe color change from yellow to brown) and UV-visible spectrometric analysis (to monitor SPR signal) to determine the ideal volumetric ratios of CSAE to AgNO<sub>3</sub> required for synthesis of pure AgNPs.

**Optimization based on pH:** The three solution mixtures were prepared and maintained at different pH 5, 7 and 8 for AgNPs synthesis. The pH of three reaction mixtures was adjusted by adding 0.1 N HCl and/or 0.1 N NaOH solutions. Each reaction mixture with different pH was subjected to visual examination (for observation of change in colour from yellow to brown) and UV-visible analysis (for monitoring of SPR peak) to determine the ideal pH required for synthesis of pure AgNPs.

**Optimization based on temperature:** Three reaction mixtures were prepared and maintained in same conditions except for temperature 5, 25 and 60 °C. The three reaction mixtures were subjected to visual examination (to monitor colour change from yellow to brown) and UV-visible analysis (to observe the SPR signal) to determine the most suitable temperature required for synthesis of pure AgNPs.

**Stability studies over synthesized AgNPs:** Stability study of synthesized AgNPs was based on the reported methods with minor modifications [4,18]. The AgNPs stability was determined based on SPR signal range (340 to 540 nm) in UV-visible absorption spectrum. The measurements for stability study were made at 0 h, 24 h, 7 days, 15 days and 30 days.

**Characterization of AgNPs:** Once the optimization and stability studies of AgNPs were completed, pure AgNPs were subjected to characterization experiments mentioned earlier [18]. Prior to characterization studies, the synthesized AgNPs were repeatedly washed and centrifuged using deionized water. Repeated washing and centrifugation process was done to avoid interference of unbound residual biochemical entities of CSAE with characterization data of biogenic AgNPs. The characterization of biogenic AgNPs was based on several analytical techniques, such as Fourier transformed infrared spectrometry (FTIR), field emission scanning electron microscopy (FESEM), X-ray diffraction (XRD) and energy-dispersive X-ray (EDX) spectrometry. Formation of AgNPs was determined based on the change in colour of solution, UV-Visible (Shimadzu U-2800) and FTIR (PerkinElmer SLE/MSC4/29) spectrometric data. The FESEM measurement was performed to understand the morphology of AgNPs using FEI Nova NanoSEM 450. The AgNPs crystal nature was determined by observing their XRD pattern using PANalytical X'Pert PRO MRD PW 3040/60 X-

ray diffractometer. XRD measurement was operated at 40 kV and 40 mA and spectrum was recorded by  $\text{CuK}\alpha\beta$  radiation with a wavelength of  $\text{\AA}$  in the  $1.54060$   $2\theta$  range of  $10^\circ$ - $80^\circ$ . The EDX measurement was performed using FEI Nova Nano-SEM 450 with EDX unit.

**Antimicrobial activity:** The synthesized AgNPs and corn silk aqueous extract (CSAE) were evaluated for antimicrobial potential against *K. pneumoniae* (ATCC 10031), *E. coli* (ATCC 8739), *S. aureus* (ATCC 29737) and *B. cereus* (ATCC 11778) using well-diffusion method [4]. Briefly, the fresh and pure culture of each bacterial strain was sub-cultured over nutrient broth (NB) at  $37^\circ\text{C}$  (previously shaken on a rotary shaker at 200 rpm). The strain of each bacterial culture was uniformly swabbed using sterile cotton over individual nutrient agar plates. Using gel puncture wells of 6 mm size were drilled on nutrient agar plates. In each well of nutrient agar plate, using micropipette were added AgNPs (100, 200, 400, 600, 800 and 1000  $\mu\text{g/mL}$ ), CSAE (10, 20, 40, 60, 80 and 100  $\text{mg/mL}$ ), and ciprofloxacin (50  $\mu\text{g/mL}$ ) each in a volume of 50  $\mu\text{L}$ . Lastly, the plates were incubated at  $37^\circ\text{C}$  for 24 h and zone of inhibitions were measured.

**Antiuro lithiatic activity:** Antiuro lithiatic (nucleation test) activity of synthesized AgNPs and corn silk aqueous extract (CSAE) against calcium oxalate crystals growth was conducted as per the procedure given in research study of Atmani and Khan [19] with slight modification. Briefly, the solutions of sodium oxalate and calcium chloride were prepared in a concentration of 7.5 mM and 5 mM, respectively, in a buffer of Tris 0.05 M and NaCl 0.15 M. The solutions were maintained at  $37^\circ\text{C}$ . Both the solutions were filtered through 0.22  $\mu\text{m}$  filter. The CSEA solution was prepared in different concentrations, such as 20, 40, 60, 80, 100  $\text{mg/mL}$  and without CSAE (control). Into the 200  $\mu\text{L}$  of each CSAE solution was added 1800  $\mu\text{L}$  of 5 mM calcium chloride solution and mixed well. Crystallization was initiated by adding 1800  $\mu\text{L}$  of sodium oxalate into each CSAE solution. All the final solutions were magnetically stirred at 800 rpm and visualized under the compound microscope to observe the formation of calcium oxalate crystals, if any. All the solutions were also subjected to the absorbance measurement using UV-visible spectrometer at 620 nm for 6 min after initiation of crystallization. The optical density (O.D.) of the solution was monitored at 620 nm. The temperature was maintained at  $37^\circ\text{C}$ . The rate of nucleation was estimated by comparing the induction time (delay before the appearance of crystals that have reached a critical size and thus become optically detectable) in the presence of the extract with that of the control (no extract). The similar protocol was repeated with different concentrations of synthesized AgNPs with concentrations of 1000, 800, 600, 400, 200 and 100  $\mu\text{g/mL}$ . Percent inhibition was calculated using the following eqn. 1:

$$\text{Crystal growth inhibition (\%)} = \frac{A_{\text{control}} - A_{\text{drug}}}{A_{\text{control}}} \times 100 \quad (1)$$

## RESULTS AND DISCUSSION

**Synthesis of AgNPs:** The AgNPs synthesis was confirmed based on visual examination and UV-visible analysis. Stirred reaction mixture of  $\text{AgNO}_3$  solution and corn silk aqueous extract

(CSAE) was kept aside at  $25^\circ\text{C}$  for monitoring of change in colour. After 24 h, a colour change from yellow to brown was observed. The brown colour solution, when subjected to UV-visible spectrometric analysis, resulted in a signal at 430 nm in the UV-visible absorption spectrum (Fig. 1) indicated the formation of AgNPs.

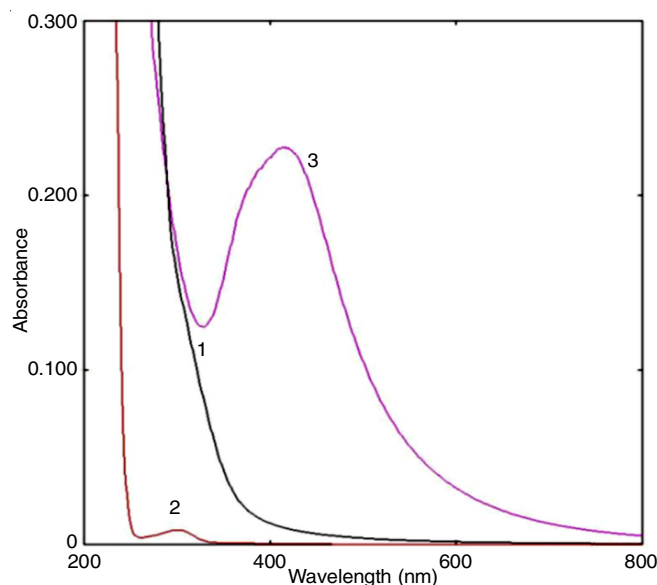


Fig. 1. UV-visible spectra indicating AgNPs synthesis

In Fig. 1, curve 3 exhibited signal at 430 nm for AgNPs, whereas curve 1 (pure CSAE) and curve 2 ( $\text{AgNO}_3$ ) exhibited no signal in AgNPs UV-visible range. The results of present study were authenticated based on presence of SPR signal within the range of results claimed by other research studies [4,20,21]. The resultant data of present study confirmed the successful synthesis of silver nanoparticles using CSAE. Synthesis of AgNPs occurred, when  $\text{AgNO}_3$  was exposed to CSAE. Visual examination of colour change from yellow to brown and absorbance signal at 430 nm in UV-visible spectrum (Fig. 1) confirmed formation of AgNPs and reduction of  $\text{Ag}^+$  to  $\text{Ag}^0$ . UV-visible signal at 430 nm was attributed to surface plasmon resonance property, conceivably a result of stimulation of longitudinal plasmon vibrations [21].

**Optimization of AgNPs synthesis:** Optimization of AgNPs synthesis involved optimization of four parameters namely:  $\text{AgNO}_3$  concentration, ratio of CSAE to silver nitrate, pH and temperature. Results were validated based on SPR peak range claimed by standard investigations [4,20,21].

**Optimization based on  $\text{AgNO}_3$  concentration:** The UV-visible analysis assisted optimization over synthesis of AgNPs based on four concentrations of  $\text{AgNO}_3$  (1, 2, 3 and 5 mM) as parameter offered a UV-visible spectrum (Fig. 2) exhibited four curves 1, 2, 3 and 4.

According to Fig. 2, curves 1, 2, and 3 (related to 1, 2, 3 mM  $\text{AgNO}_3$ , respectively) did not showed any signal in the range of 435-450 nm. Whereas curve 4 (related to 5 mM  $\text{AgNO}_3$ ) exhibited a signal at 430 nm representing formation of AgNPs. The SPR signal at 430 nm displayed in curve 4 revealed the formation of AgNPs. Hence, 5 mM of  $\text{AgNO}_3$  concentration was considered as an optimum requirement for synthesis of

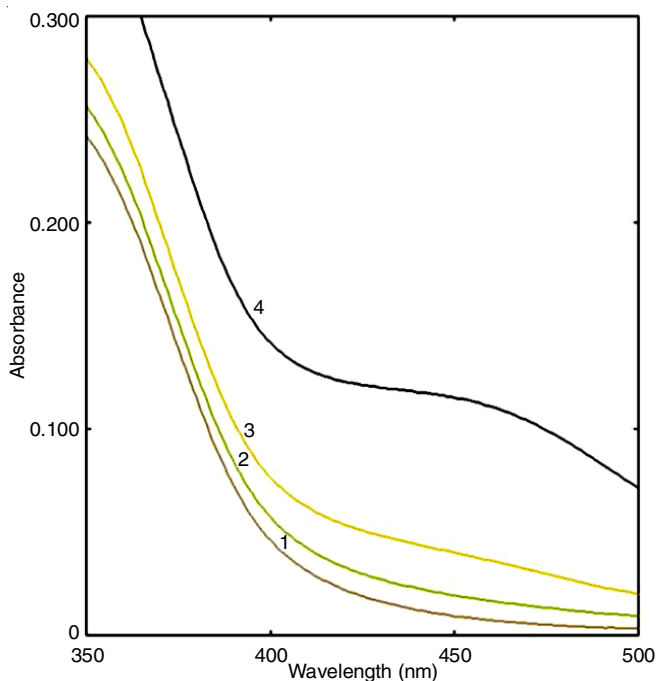


Fig. 2. UV-visible spectra indicating AgNPs synthesis based on  $\text{AgNO}_3$  concentration

AgNPs using CSAE. Optimization results for  $\text{AgNO}_3$  concentration (5 mM) in present study were confirmed by observing the SPR signal range of other research in similar range [4,20,21].

**Optimization based on volumetric ratios of CSAE to  $\text{AgNO}_3$ :** The optimization of synthesis of AgNPs based on five volumetric ratios of CSAE to  $\text{AgNO}_3$  (1:9, 1.5:8.5, 2:8, 2.5:7.5 and 5:5) as parameter generated UV-visible absorption spectrum (Fig. 3) exhibited five curves 1, 2, 3, 4 and 5.

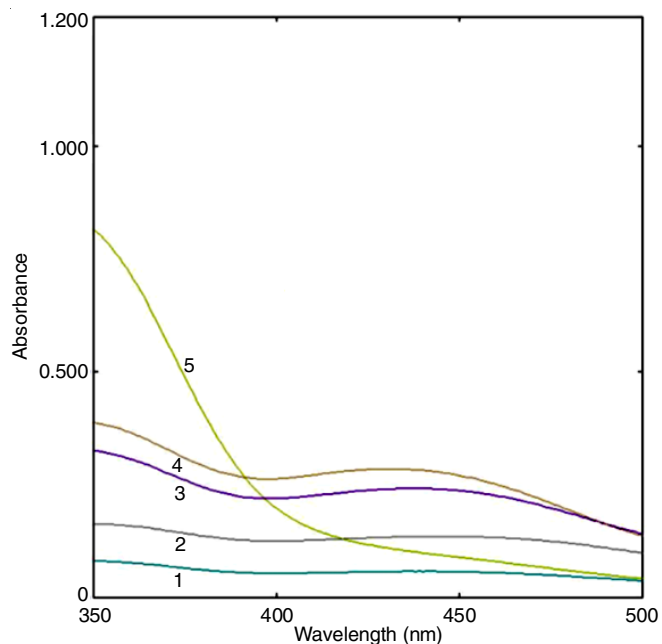


Fig. 3. UV-visible spectra indicating AgNPs synthesis based on CSAE/ $\text{AgNO}_3$  ratio

Among the five curves, presence of SPR signal at 430 nm was observed in curve 3 and 4, which indicated the completion of AgNPs synthesis. Curve 4 showed a higher absorbance of

SPR signals than curve 3. Among the 2:8 and 2.5:7.5 CSAE to  $\text{AgNO}_3$  ratio, the 2.5:7.5 ratio showed higher absorbance value at 430 nm, hence, 2.5:7.5 ratio of CSAE to  $\text{AgNO}_3$  was considered as optimum for synthesis of AgNPs. The optimization study results for volumetric ratio of CSAE and  $\text{AgNO}_3$  (2.5:7.5) to display signal at 430 nm was confirmed by observing the SPR signal range of other research studies [4,20,21].

**Optimization based on pH:** The UV-visible experiment aided optimization study over synthesis of AgNPs based on three pHs (pH 5, 7 and 8) yielded a UV-Visible spectrum (Fig. 4) exhibiting three curves 1, 2 and 3. The UV-visible spectrum displayed no absorption signal for AgNPs in curve 1 (related to pH 5). The spectrum displayed SPR signal for AgNPs in curve 2 and 3 (related to pH 7 and pH 8) at 430 nm indicating the completion of synthesis of AgNPs. The UV-visible spectrum (Fig. 4) revealed that pH 5 (curve 1) was unsuitable to formulate AgNPs. Whereas, pH 7 and 8 (curve 2 and 3) were ideal to produce AgNPs displaying signal at 430 nm. Hence, maintaining the reaction at pH 7 and 8 was considered as optimum for AgNPs synthesis. The absorbance of curve 3 was higher indicated that pH 8 was more ideal to synthesize the AgNPs using CSAE. The pH optimization results for synthesis of AgNPs in present study were verified by observing the similar SPR signal range of other studies [4,20,21].

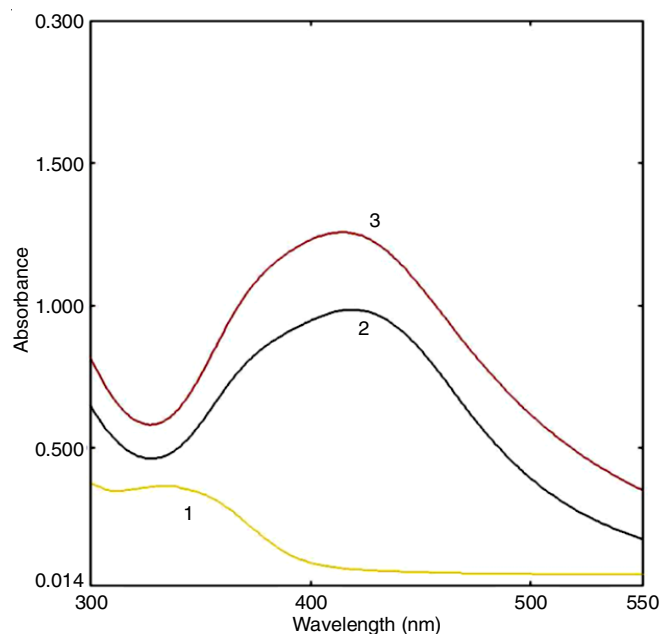


Fig. 4. UV-visible spectra indicating AgNPs synthesis based on pH

**Optimization based on temperature:** The UV-visible study over AgNPs synthesis based on optimization of temperature (5 °C, room temperature (25 °C) and 60 °C) produced a UV-visible spectrum (Fig. 5) exhibiting three curves 1, 2 and 3.

The UV-visible spectrum (Fig. 5) displayed no absorption signals in curve 2 (at 5 °C). The spectrum with absorption signal for AgNPs in curve 1 and 3 (at 25 and 60 °C) at 360 and 440 nm revealed completion of synthesis of AgNPs. The absorption spectrum (Fig. 5) revealed that 5 °C (curve 2) was not ideal to formulate AgNPs, whereas, 25 and 60 °C (curve 1 and 3) were ideal temperature to produce AgNPs. Among curves

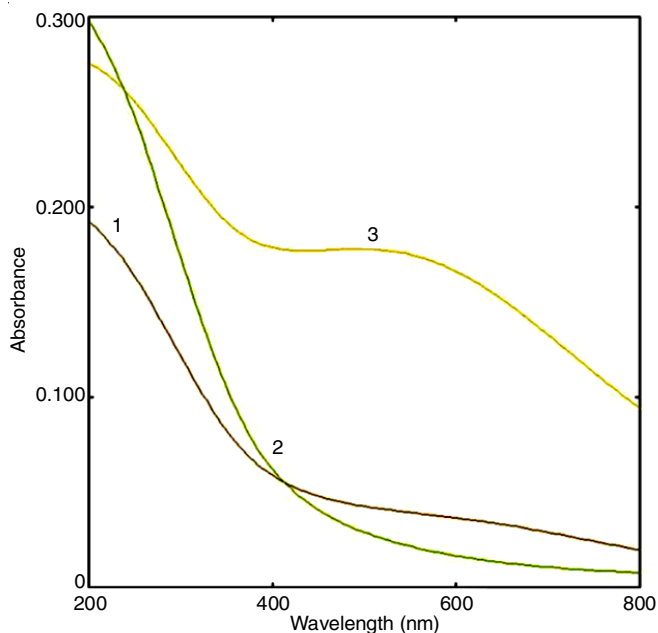


Fig. 5. UV-visible spectra indicating AgNPs synthesis based on temperature

1 and 3, curve 3 showed higher absorbance at 440 nm, hence the reaction at 60 °C was considered as optimum for AgNPs synthesis using CSAE. The results of optimization study over AgNPs synthesis were also supported by other literary evidences [4,20,21].

**Stability study for biogenic AgNPs:** The UV-visible spectrometry assisted in the stability study of synthesized AgNPs. The stability study was conducted for 0 h, 24 h, 7 days, 15 days and 30 days. The UV-visible absorption spectrum (Fig. 6) of AgNPs containing 1, 2, 3, 4 and 5 curves for 0 h, 24 h, 7 days, 15 days and 30 days, respectively.

Fig. 6 illustrated the retention of AgNPs signal in the range of 428 to 450 nm. The spectrum exhibited increase in absorbance of AgNPs with time and represented AgNPs stability after 30 days due to retention of AgNPs signal in the range of 428 to 450 nm. The present study AgNPs signal range was also supported by other research studies [4].

**FTIR analysis:** The FTIR characterization aided in the determination of  $\text{Ag}^+$  to  $\text{Ag}^0$  reduction and AgNPs formation [4]. The FT-IR spectrum of CSAE (Fig. 7) displayed the characteristic bands at  $3467\text{ cm}^{-1}$  (O-H vibrations),  $2926$  and  $2877\text{ cm}^{-1}$  (C-H vibrations),  $1704\text{ cm}^{-1}$  (C=O vibrations). The FTIR spectrum for AgNPs (Fig. 8) displayed the shifted bands  $3472\text{ cm}^{-1}$  (O-H vibrations),  $2927$  and  $2879\text{ cm}^{-1}$  (C-H vibra-

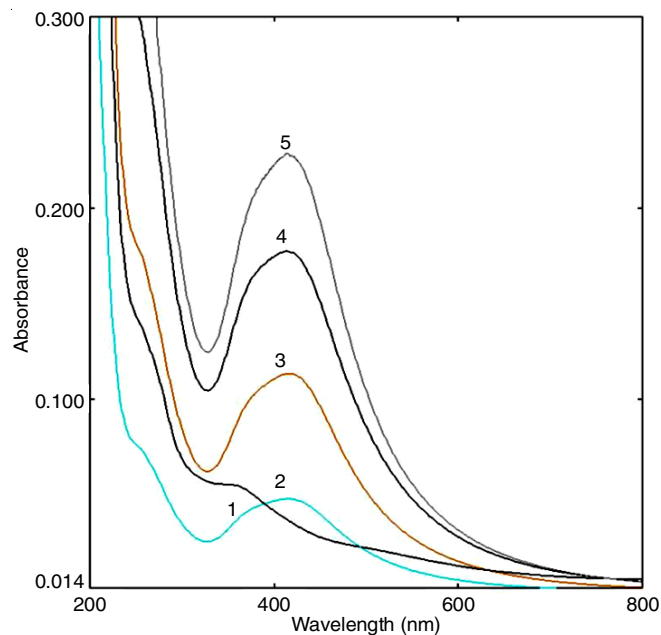


Fig. 6. UV-visible spectrum indicating stability of AgNPs

tions),  $1706\text{ cm}^{-1}$  (C=O vibrations). Resultant data indicated the formation of AgNPs and reduction of  $\text{Ag}^+$  to  $\text{Ag}^0$ . The CSAE was recognized as dual capping (stabilizing) and reducing agent based on the comparison of FTIR spectrum of CSAE and synthesized AgNPs. The FTIR spectrum of CSAE as it retained majority of signals with marginal shifting and broadening. For example,  $3467.21\text{ cm}^{-1}$  (O-H vibrations) narrow band in FTIR spectrum of CSAE (Fig. 7) was shifted to  $3472.33\text{ cm}^{-1}$  as a broad band in FTIR spectrum of AgNPs (Fig. 8).

The literature revealed that corn silk consisted of various chemicals such as proteins, vitamins, alkaloids, tannins, phenolic compounds like anthocyanins, *p*-coumaric acid, vanillic acid, procatechuic acid, derivatives of hisperidin and quercetin. It is also very rich in flavonoids including maysin and rutin [22]. The FTIR spectrum of biogenic AgNPs of the present study revealed that an interaction of biochemical moieties of CSAE with AgNPs caused broadening and marginal shifting of IR band signal positions relatively. This recognized the dual role of CSAE both as reducing and stabilizing agent [4,23]. The resultant broadening and shifting of absorption bands in FTIR spectrum of AgNPs in comparison to pure CSAE was also supported by other investigations [24,25].

**FESEM analysis:** The FESEM micrographs (Fig. 9) indicated that synthesized AgNPs were well dispersed, spherical

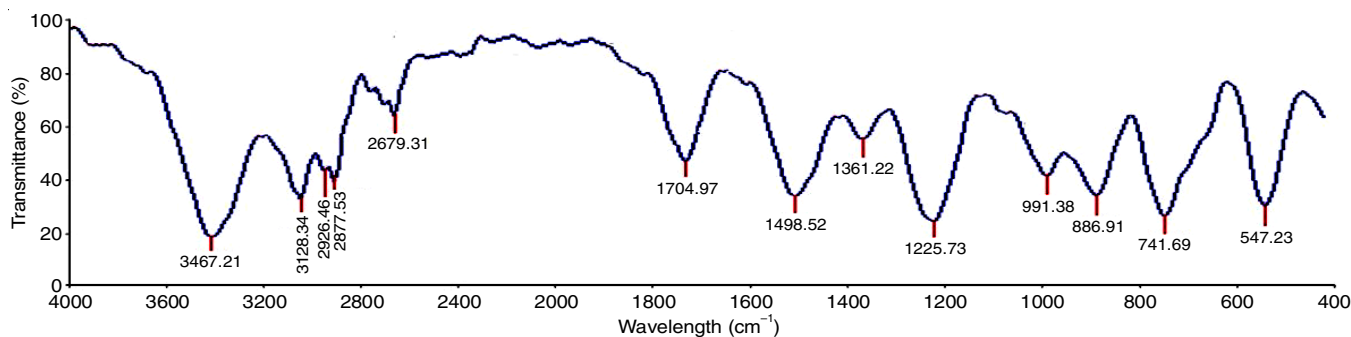


Fig. 7. FTIR spectra of pure CSAE

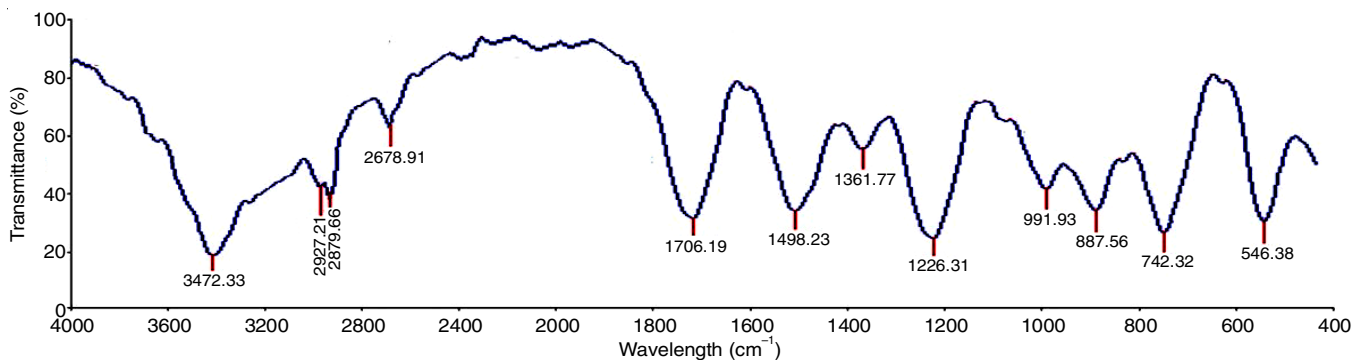


Fig. 8. FTIR spectra of pure biosynthesized AgNPs

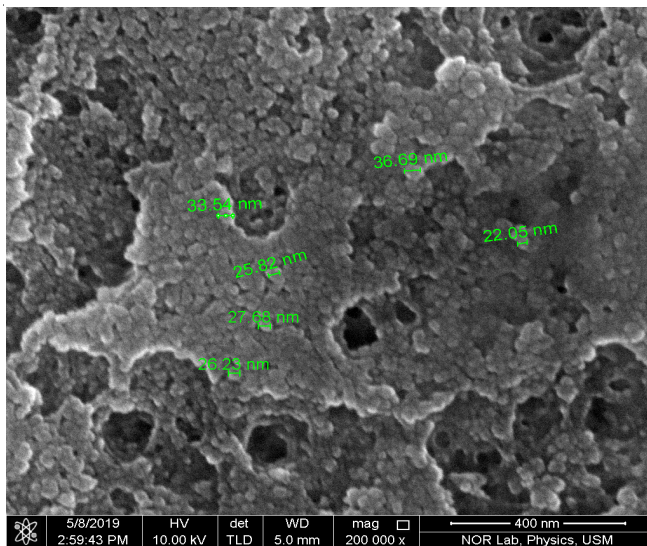


Fig. 9. FESEM image of AgNPs

shaped and ranged between 22.05-36.69 nm in size and resulted by complete reduction of silver from silver nitrate solution by CSAE.

**XRD analysis:** The analysis of XRD pattern (Fig. 10) showed the distinctive diffraction peaks at  $2\theta$  values of  $32.27^\circ$ ,  $40.72^\circ$ ,  $46.20^\circ$ ,  $65.69^\circ$ ,  $69.31^\circ$  and  $76.49^\circ$  designated to (111), (200), (220) and (311) reflection planes of the face-centered cubic structure of silver. By using the Debye-Scherrer formula, an average crystallite size of nanoparticles was found to be in the range of 31.9-55.44 nm. The XRD pattern results of present study were verified by other standard studies [4,23].

**EDX analysis:** The EDX spectrum of AgNPs (Fig. 11) exhibited silver (62.17%) as a major constituent element compared

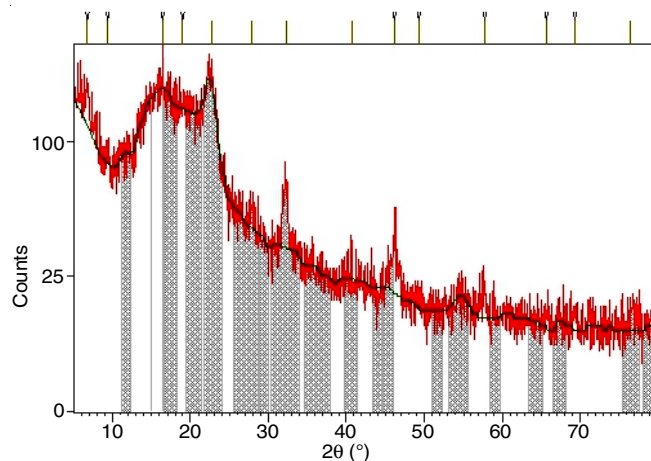


Fig. 10. XRD spectrum of AgNPs

to carbon (13.45%), oxygen (5.5%), nitrogen (4.14%), chlorine (14.99%). Generally, metallic silver nanoparticle shows their typical optical absorption peak approximately at 3 KeV [26,27]. The EDX spectrum showed a strong signal for silver along with weak oxygen peak which may be attributed to the bio-molecules that were bound to the surface of silver nanoparticles, indicating the reduction of silver ions to elemental silver.

**Antimicrobial activity of AgNPs:** The AgNPs have extensive use being an antimicrobial and registered as more potent in comparison to silver ions [28,29]. The resultant data given in Table-1 revealed that inhibition zone of synthesized AgNPs was much higher than pure CSAE. When compared to ciprofloxacin, newer AgNPs exhibited a maximum zone of inhibition against *S. aureus* (18.6 mm at 0.5 mg/mL and 22.8 mm at 1 mg/mL) and *K. pneumoniae* (18.3 mm at 0.5 mg/mL and 20.0 mm at 1 mg/mL). The AgNPs displayed lesser zone of inhibition

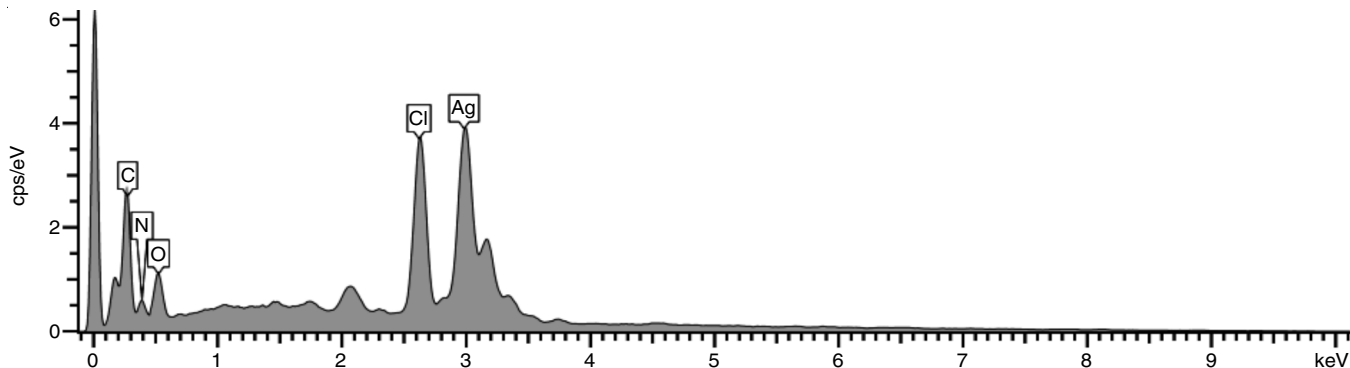


Fig. 11. EDX spectrum of AgNPs

TABLE-1  
ZONE OF INHIBITION (EXPRESSED IN mm)

Microorganism	Zone of inhibition (mm)												
	Silver nanoparticles						Corn silk aqueous extract					Ciprofloxacin	
Conc. ( $\mu\text{g/mL}$ )	10	20	40	60	80	100	10	20	40	60	80	100	50
<i>B. cereus</i>	13.5	13	14.5	15.7	17.0	17.0	N/A	N/A	N/A	N/A	N/A	N/A	21
<i>S. aureus</i>	13.6	16.5	20.1	18.6	19.9	22.8	N/A	N/A	N/A	N/A	N/A	N/A	21
<i>E. coli</i>	13.8	15.2	16.5	18.6	18.8	18.9	N/A	N/A	N/A	N/A	N/A	N/A	20
<i>K. pneumoniae</i>	13.1	15.2	17.5	18.3	18.3	20.0	N/A	N/A	N/A	N/A	N/A	N/A	21

N/A: No activity

against *E. coli* (18.6 mm at 0.5 mg/mL and 18.9 mm at 1 mg/mL) and *B. cereus* (15.7 mm at 0.5 mg/mL and 17.0 mm at 1 mg/mL). In comparison to AgNPs, pure CSAE exhibited no zone of inhibition against *E. coli*, *S. aureus*, *K. pneumoniae* and *B. cereus*. Interestingly, a pattern was observed in the antimicrobial activity of newer AgNPs, when the concentration of AgNPs was increased from 0.1 mg/mL to 1 mg/mL, there was a significant increase in the zone of inhibition. The antimicrobial activity results indicated that capping of silver with biochemical moieties of CSAE (sugars, proteins, coumarins, anthraquinones, saponin glycosides, flavonoids, alkaloids, tannins and phenolic compounds) caused a marked increase in the antimicrobial potential of AgNPs. This pattern of increment in antimicrobial response due to biochemical moieties of plant extract (used for the synthesis of silver nanoparticles) is also supported by other investigations [24]. Other investigations also supported that AgNPs smaller in size and higher in dose exhibits higher antimicrobial potential [30,31].

As per the antimicrobial results of present study and literary evidences [32], it can be postulated that biochemical moieties of CSAE caused capping of silver and lead to marked increase in antimicrobial potential of AgNPs against periodontitis causing pathogenic microbiota.

**Antirolithiatic activity of synthesized AgNPs against calcium oxalate crystals growth:** Fig. 12 exhibited the positive antirolithiatic activity of biogenic AgNPs as they inhibited the crystallization of calcium oxalate and prevented nucleation. The antirolithiatic potential of CSAE and AgNPs in different concentrations was also supported by observing the microscopic view. There were smaller and lesser particles when the concentration of AgNPs was increased from lower to higher. Fig. 13 represents the microscopic view (nucleation) of calcium

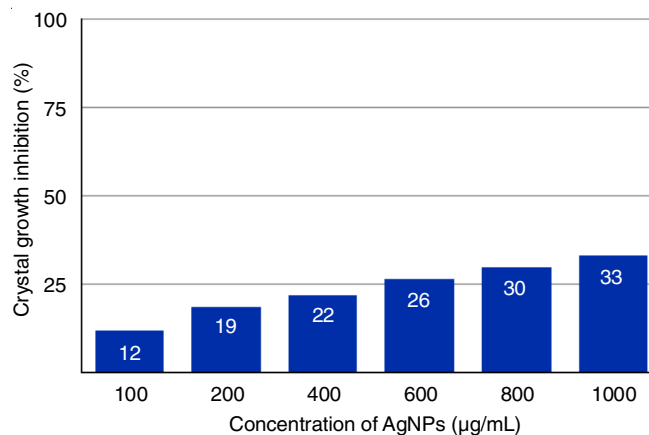


Fig. 12. Crystal growth inhibition by biosynthesized AgNPs

oxalate crystals in solution without CSAE (A), with CSAE 100 mg/mL (B) and with 1000  $\mu\text{g/mL}$  AgNPs (C).

Hence, based on the antirolithiatic results offered by the AgNPs blended with CSAE, it can be postulated that AgNPs synthesized using CSAE would be advantageous in prevention of urinary stone formation by promoting the excretion of small particles from the kidney. Although further *in vivo* studies are yet to be done, but present study provides the basis over antirolithiatic potential of AgNPs synthesized using CSAE.

## Conclusion

The visual examination, UV-visible and FTIR data of the present study confirmed the success of synthesis of silver nanoparticles using corn silk aqueous extract (CSAE). The FESEM, EDX and XRD data established that AgNPs were well dispersed, spherical shaped, crystalline nature and their size ranged from 22.05-36.69 nm. The biological investigations of present study

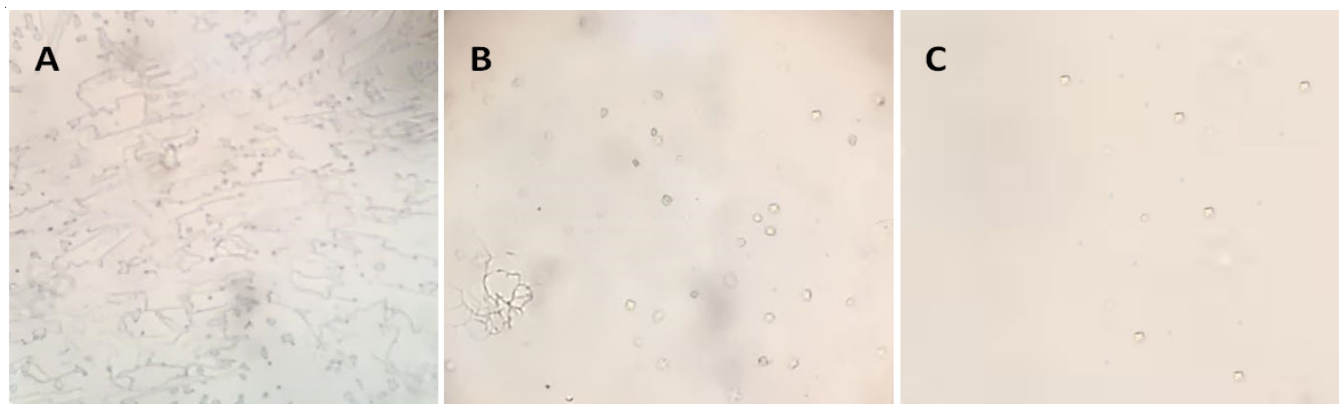


Fig. 13. Microscopic view of calcium oxalate crystals in solution without CSAE (A), with CSAE 100 mg/mL (B) and with 1000  $\mu\text{g/mL}$  AgNPs (C)

conclude silver nanoparticles to possess substantial antimicrobial and antiuro lithiatic potential; and recommends corn silk aqueous extract (CSAE) as a potential source for production of silver nanoparticles.

### ACKNOWLEDGEMENTS

The authors are thankful to Nano Optoelectronic Research and Technology (NOR) Lab, School of Physics, Universiti Sains Malaysia for assisting in spectral analysis.

### CONFLICT OF INTEREST

The authors declare that there is no conflict of interests regarding the publication of this article.

### REFERENCES

- C. Fisang, R. Anding, S.C. Muller, S. Latz and N. Laube, *Dtsch. Arztebl. Int.*, **112**, 83 (2015); <https://doi.org/10.3238/arztebl.2015.0083>
- P. Das, K. Kumar, A. Nambiraj, R. Rajan, R. Awasthi, K. Dua and M. Himaja, *Int. J. Biol. Macromol.*, **103**, 621 (2017); <https://doi.org/10.1016/j.ijbiomac.2017.05.096>
- P. Das, K. Kumar, A. Nambiraj, R. Awasthi, K. Dua and H. Malipeddi, *Recent Pat. Drug Deliv. Formul.*, **12**, 170 (2019); <https://doi.org/10.2174/1872211312666180723160624>
- N.K. Fuloria, S. Fuloria, K.Y. Chia, S. Karupiah and K. Sathasivam, *J. Appl. Biol. Biotechnol.*, **7**, 1 (2019); <https://doi.org/10.7324/JABB.2019.70408>
- T.C. Dakal, A. Kumar, R.S. Majumdar and V. Yadav, *Front. Microbiol.*, **7**, 1831 (2016); <https://doi.org/10.3389/fmicb.2016.01831>
- C.E. Escárcega-González, J.A. Garza-Cervantes, A. Vazquez-Rodríguez, L.Z. Montelongo-Peralta, M.T. Treviño-Gonzalez, E. Díaz Barriga Castro, E.M. Saucedo-Salazar, R.M. Chávez Morales, D.I. Regalado-Soto, F.M. Treviño-González, J.L. Carrasco-Rosales, R. Villalobos-Cruz and J.R. Morones-Ramirez, *Int. J. Nanomedicine*, **13**, 2349 (2018); <https://doi.org/10.2147/IJN.S160605>
- A.E. Mohammed, A. Al-Qahtani, A. Al-Mutairi, B. Al-Shamri and K. Aabed, *Nanomaterials*, **8**, 382 (2018); <https://doi.org/10.3390/nano8060382>
- Y.Y. Loo, Y. Rukayadi, M.-A.-R. Nor-Khaizura, C.H. Kuan, B.W. Chieng, M. Nishibuchi and S. Radu, *Front. Microbiol.*, **9**, 1555 (2018); <https://doi.org/10.3389/fmicb.2018.01555>
- J. Venkatesan, S.K. Singh, S. Anil, S.K. Kim and M.S. Shim, *Molecules*, **23**, 1429 (2018); <https://doi.org/10.3390/molecules23061429>
- A. Mehmood, G. Murtaza, T.M. Bhatti and R. Kausar, *Acta Metal. Sinica*, **27**, 75 (2014); <https://doi.org/10.1007/s40195-014-0025-7>
- M. Gomathi, P. Rajkumar, A. Prakasam and K. Ravichandran, *Resour. Efficient Technol.*, **3**, 280 (2017); <https://doi.org/10.1016/j.reffit.2016.12.005>
- S. Jain and M.S. Mehata, *Sci. Rep.*, **7**, 15867 (2017); <https://doi.org/10.1038/s41598-017-15724-8>
- J. Mittal, R. Jain and M.M. Sharma, *Adv. Nat. Sci.: Nanosci. Nanotech.*, **8**, 025011 (2017); <https://doi.org/10.1088/2043-6254/aa6879>
- K.J. Wang and J.L. Zhao, *Biomed. Pharmacother.*, **110**, 510 (2019); <https://doi.org/10.1016/j.biopha.2018.11.126>
- A.B.L.D. Carvalho, C.A. Cruz, C.L.A.D. Freitas, J.J.D.S. Aguiar, P.L.W. D.S. Nunes, V.M.D.S. Lima, E.F.F. Matias, D.F. Muniz and H.D.M. Coutinho, *Antibiotics*, **8**, 22 (2019); <https://doi.org/10.3390/antibiotics8010022>
- A.W. Ha, H.J. Kang, S.L. Kim, M.H. Kim and W.K. Kim, *Prev. Nutr. Food Sci.*, **23**, 70 (2018); <https://doi.org/10.3746/pnf.2018.23.1.70>
- N. Tanideh, F. Zarifi, S. Rafiee, M. Khastkhodaei, O.K. Hosseinabadi, F. Tarkesh, Z. Kherad, M.M. Taghi, M. Kamali, G. Shekarkhar, M. Jahromi and F. Zarifi, *Galen Med. J.*, **7**, 1258 (2018); <http://dx.doi.org/10.22086/gmj.v0i0.1258>
- S. Fuloria, N.K. Fuloria, C.J. Yi, T.M. Khei, T.A. Joe, L.T. Wei, S. Karupiah, N. Paliwal, K. Sathasivam, *Bull. Environ. Pharmacol. Life Sci.*, **8**, 112 (2019).
- F. Atmani and S.R. Khan, *BJU Int.*, **85**, 621 (2000); <https://doi.org/10.1046/j.1464-410x.2000.00485.x>
- J.K. Patra and K.-H. Baek, *Front. Microbiol.*, **8**, 167 (2017); <https://doi.org/10.3389/fmicb.2017.00167>
- P. Logeswari, S. Silambarasan and J. Abraham, *Sci. Iran.*, **20**, 1049 (2013).
- M.A. Ebrahimzadeh, M. Mahmoudi, N. Ahangar, S. Ehteshami, F. Ansaroudi, S.F. Nabavi, S.M. Nabavi and I. Sari, *Pharmacologyonline*, **3**, 347 (2009).
- K. Anandalakshmi, J. Venugobal and V. Ramasamy, *Appl. Nanosci.*, **6**, 399 (2016); <https://doi.org/10.1007/s13204-015-0449-z>
- M. Shaik, M. Khan, M. Kuniyil, A. Al-Warthan, H. Alkhatlan, M. Siddiqui, J. Shaik, A. Ahamed, A. Mahmood, M. Khan and S. Adil, *Sustainability*, **10**, 913 (2018); <https://doi.org/10.3390/su10040913>
- H. Erjaee, H. Rajaian and S. Nazifi, *Adv. Nat. Sci.: Nanosci. Nanotech.*, **8**, 025004 (2017); <https://doi.org/10.1088/2043-6254/aa690b>
- A. Deljou and S. Goudarzi, *Iranian J. Biotechnol.*, **14**, 25 (2016); <https://doi.org/10.15171/ijb.1259>
- A.S. Dakhil, *J. King Saud. Univ. Sci.*, **29**, 462 (2017); <https://doi.org/10.1016/j.jksus.2017.05.013>
- J. Sudiono, F. Sandra, N.S. Halim, T.A. Kadrianto and M. Melinia, *Dent. J. Majal. Ked. Gig.*, **46**, 9 (2013); <https://doi.org/10.20473/j.djmk.v46.i1.p9-13>
- X. Yan, B. He, L. Liu, G. Qu, J. Shi, L. Hu and G. Jiang, *Metallomics*, **10**, 557 (2018); <https://doi.org/10.1039/C7MT00328E>
- S. Gurunathan, Y.J. Choi and J.H. Kim, *Int. J. Mol. Sci.*, **19**, 1210 (2018); <https://doi.org/10.3390/ijms19041210>
- E. Pazos-Ortiz, J.H. Roque-Ruiz, E.A. Hinojos-Márquez, J. López-Esparza, A. Donohué-Cornejo, J.C. Cuevas-González, L.F. Espinosa-Cristóbal and S.Y. Reyes-López, *J. Nanomater.*, **2017**, 1 (2017); <https://doi.org/10.1155/2017/4752314>
- R. Emmanuel, S. Palanisamy, S.-M. Chen, K. Chelladurai, S. Padmavathy, M. Saravanan, P. Prakash, M.A. Ali and F.M.A. Al-Hemaid, *Mater. Sci. Eng. C*, **56**, 374 (2015); <https://doi.org/10.1016/j.msec.2015.06.033>